ISBN: 978-3-95450-227-1 ISSN: 2673-5490 doi:10.18429/JACoW-IPAC2022-THPOST026

DESIGN OF THE MAGNETIC SHIELD FOR VSR DEMO

H.-W. Glock†, P. Anumula, F. Glöckner, J. Knobloch[1], F. Pfloksch, A. Velez[2]
Helmholtz-Zentrum Berlin für Materialien und Energie, Berlin, Germany
[1]also at University of Siegen, Siegen, Germany
[2]also at Technical University Dortmund, Dortmund, Germany

Abstract

The VSR DEMO module, recently under development at Helmholtz-Zentrum Berlin (HZB), will house two 4-cell 1.5 GHz superconducting RF cavities with a particularly powerful HOM damping scheme based on five waveguide HOM absorbers per cavity. A magnetic shield made of high-permeable material is needed around the cavities in order to prevent the ambient magnetic field exceeding very few µT thereby causing considerable unwanted RF losses. The shield needs to accommodate the waveguides, the fundamental power coupler, two beam pipes, two He feed / return lines, the tuner and the support structures, whilst being manufacturable and mountable. The paper discusses those difficulties and presents the matured magnetic shield design. Numerical simulations are used to evaluate the efficacy of the shield.

THE VSR DEMO MODULE

VSR Demo

VSR Demo, recently under construction at HZB, aims to demonstrate the technical feasibility of a beam-ready cryo-module [1] (cf. Fig. 1) featuring two 1.5 GHz superconducting RF (SRF) cavities designed for strong bunch length modulation in the storage ring of the 3rd generation, 300 mA synchrotron light source BESSY II.

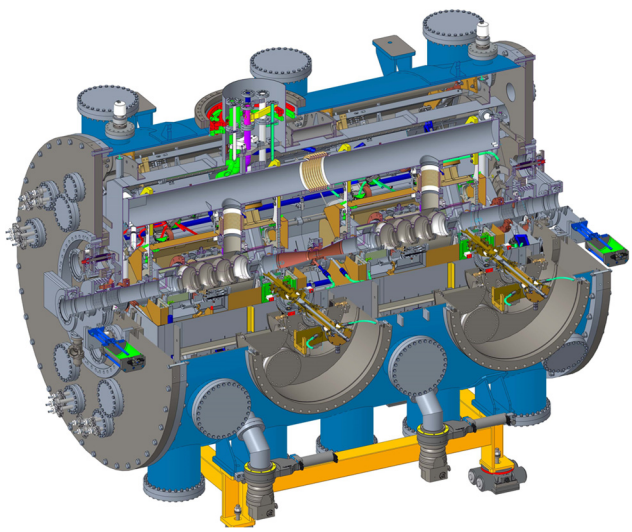

Figure 1: The VSR Demo module with two 4-cell 1.5 GHz SRF cavities.

This module will be used as a demonstrator for a later 4-cavity BESSY-VSR-module (Variable bunch length Storage Ring) [2], designed with two additional 1.75 GHz SRF cavities, which will allow to simultaneously offer long and short bunches in a fill pattern.

Main Properties Impacting the Shield Design

The high average beam current and its broad spectral distribution will cause a mean deposited wake power above 1 kW per cavity. In order to provide sufficient damping, each cavity will be equipped with five waveguides, terminated inside the cryo-module with specifically developed water-cooled HOM-absorbing loads [3]. Each cavity will be equipped with a coaxial fundamental power coupler (FPC) and an individual liquid helium (LHe) tank with a filling pipe and a gas-return pipe (GRP) connection on top. Together with the two beam pipe connections of each cavity a magnetic shield needs to accommodate in total 10 voids, most of them of significant size. That early revealed the need of at least two layers of magnetic shielding.

The LHe tank of each cavity is surrounded by a stepping-motor driven blade tuner, which allows to adjust the cavity's resonant frequency by extending its length by 0 … 1.2 mm. The inner shield, which for the reason of tuner accessibility needed to be mounted in between the tuner and the LHe tank, has to comply with such a length variation. A circumferential slit with coaxially overlapping parts, even though unfavourably reducing the shielding efficacy, was seen as the best engineering solution. The tuner stepping motor is considered as a potential source of permanent or low-frequency magnetic fields, therefore (and for easier access) it is placed outside the secondary magnetic shield.

In order to preserve the distance between the cavities during cool-down a set of four Invar-rods is used. Those are designed to attach the cavity supports and are placed around the cavity in parallel to the cavity axis. Invar is a special iron-nickel-alloy (Fe64Ni36) which experiences (almost) no thermal shrinkage. It is also a soft-magnetic material with a relative permeability μ_r found from supplier specification in a wide range of 1400…1800 [4] up to 4900 ... 12000 [5], very likely depending on the actual forming and annealing history of the samples; some rare measurements are given in [6], there a μ_r of 2420 was reported. The material is also known to be prone to non-negligible magnetic remanence, even though very few experimental data seem to be available [7].

* work supported by grants of the Helmholtz Association
† hans.glock@helmholtz-berlin.de

ISBN: 978-3-95450-227-1 ISSN: 2673-5490 doi:10.18429/JACoW-IPAC2022-THPOST026

SIMULATION APPROACH

The geometric complexity of the multi-component shielding structure would have caused prohibitively lengthy simulations if the non-linear permeability of typical high-μ shielding materials would have been considered. Instead a constant permeability $\mu_{num} = 10^4$ was assumed, which underestimates practical values by at least a factor of 3, often more. This allows for a significant magnetic saturation (which is not computed in the linear approach) without overestimating the shielding effect. Linearity made it furthermore possible to restrict ourselves to three main field vectors (x: cavity axis, y: ground surface normal, z: in parallel to the FPC axis). Homogeneous exterior fields of 50 μT were assumed in independent runs for each coordinate axis. This may underestimate ambient fields at the foreseen first VSR Demo testing site, where strongly varying fields, partially above 100 μT were seen in preliminary observations, but it is higher than in the BESSY II tunnel. Simulations were done with the magnetostatic solver of the CST©Suite [8]. In Fig. 2 all magnetic elements used in the simulation are shown, together with the main non-magnetic elements to illustrate geometrical relationships. Because of the availability of most shielding materials, cost and weight considerations a shield material thickness of 1 mm was assumed everywhere.

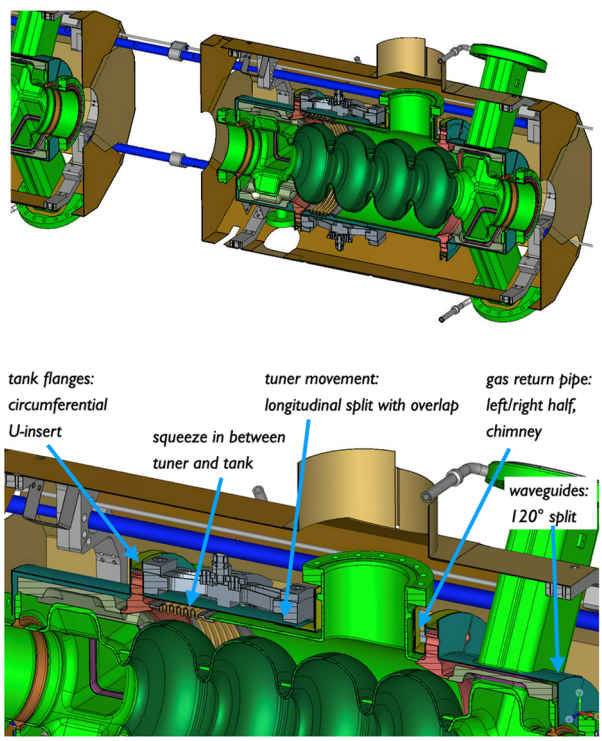

Figure 2: Simulated magnetic elements: outer (brown) and inner (dark blue-green) magnetic shield, Invar rods (blue). Non-magnetic elements shown for illustration: Cavity cells (dark green), cavity end groups and tank (green), tank flange parts (red), tuner (dark grey), supporting elements (grey). Details of critical areas of the inner shield (below).

DETAILS OF THE SHIELD LAYOUT

Inner Shield

The inner shield (cf. Fig. 3) needs to be compatible with:

- a 3-fold split of the exterior parts (120° coverage) to be mountable between waveguides, FPC and beam pipes;
- 2 x 2 parts of 180° coverage of the interior parts to be mountable around the LHe tank, ...
- …, also allowing for cavity/tank length variations;
- a sufficient overlap at all separation lines;
- a gap-free coverage of the tank flanges (thickness 15 mm) with a void in the tuner mounting area;
- a 2-fold chimney to limit the field penetration at the GRP port.

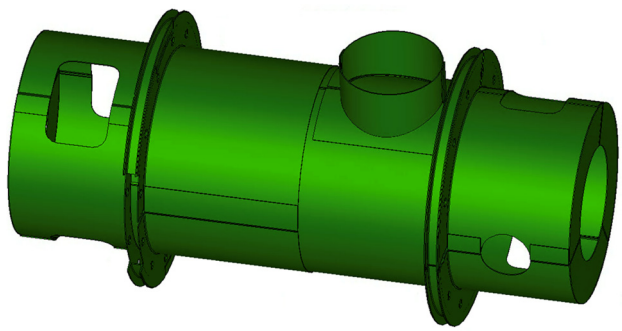

Figure 3: Components of the inner shield.

This inevitably causes a complex setup of in total 16 shield elements. In order to reduce the influence of gaps at the element boundaries, large overlaps are foreseen, which can be mounted in a way that direct metallic contact between neighbouring parts is established. The central circumferential gap is exempted from this approach, since cavity tuning, provided by the tuner-driven variation of the cavity length, would cause friction of the contacting parts. Therefore an “air”-gap cannot be avoided here, which reduces the shielding effect significantly. In order to estimate the effect, a simplified model was studied, comparing longitudinal overlaps of different lengths, assuming a radial gap width of 1 mm (cf. Fig. 4).

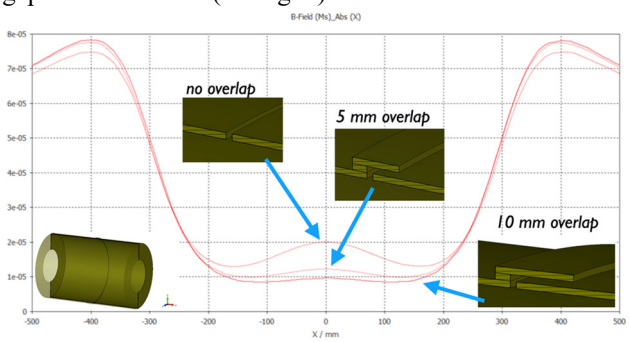

Figure 4: On-axis longitudinal B-field/T simulated for an exterior longitudinal field of 50 μT applied to the model system (lower left corner). Remaining field for 10 mm longitudinal overlap results to 10 μT, but longer overlap will not improve very much further.

ISBN: 978-3-95450-227-1 ISSN: 2673-5490 doi:10.18429/JACoW-IPAC2022-THPOST026

Outer Shield

The outer shield (cf. Fig. 5) has to provide the same set of voids for waveguide extensions like the inner one. Additionally the Invar support system connecting both cavities needs to be evaded. This demands for a fourfold split of the end-caps. Since the outer shield is not directly fixed at the cavity's tank, it needs a dedicated support, which is foreseen to be made out of a cryo-compatible fiber-enforced plastic ("G10"), also featuring highly permeable inserts helping to bridge magnetic "air" gaps between different parts. The exterior support decouples the outer shield from variations of the cavity length, which avoids the circumferential slit. Particular attention was given to the shielding of the tuner motor for which a dedicated shield perforation was designed (cf. Fig. 5 lower left).

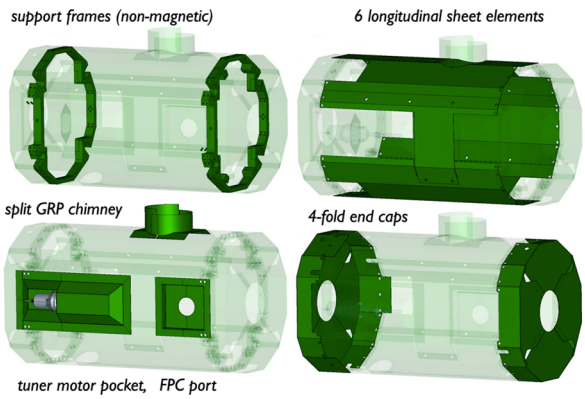

Figure 5: Highlighted details of the outer shield.

Optional Third Layer Shield

As it came clear that a two-layer shield may be not sufficient, a draft for a third layer directly inserted close to the inner surface of the module tank was included as option in the simulations. This component was not finally engineered since experimental results from the two-layer configuration shall be evaluated first. Nevertheless other module elements are constructed in a way to keep the option. The draft design as used in the simulation is shown in Fig. 6.

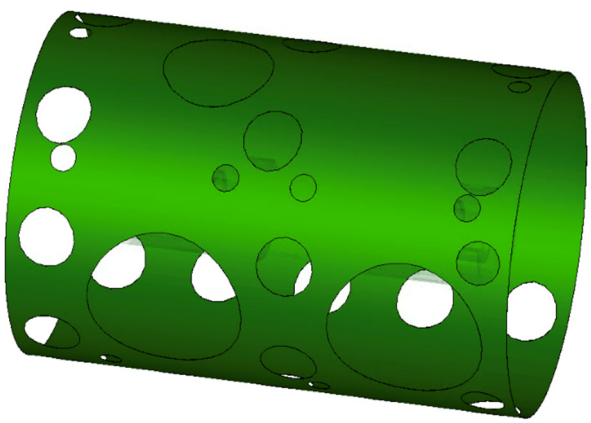

Figure 6: Optional third layer shield.

SIMULATION RESULTS

The simulation results (cf. Figs. 7 and 8) are shown separately for the three ambient external field direction as color-scaled |**B**| values. It is the aim to reach field levels lower than 1 µT in particular at the walls of the cavities' accelerating cells, in order to reliably avoid cavity Q-degradations because of trapped flux.

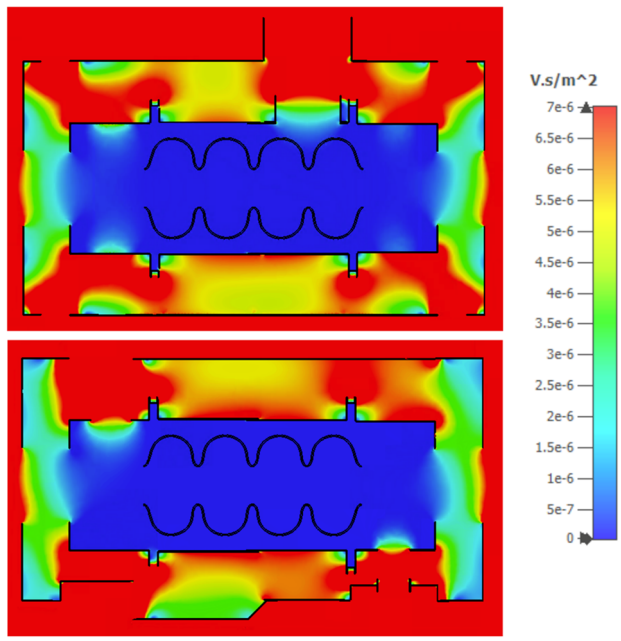

Figure 7: |**B**| for 50 µT ambient exterior field in y- (top, shown in x-y-plane) and z-direction (bottom, shown in y-z-plane). Dark blue areas are below 1 µT.

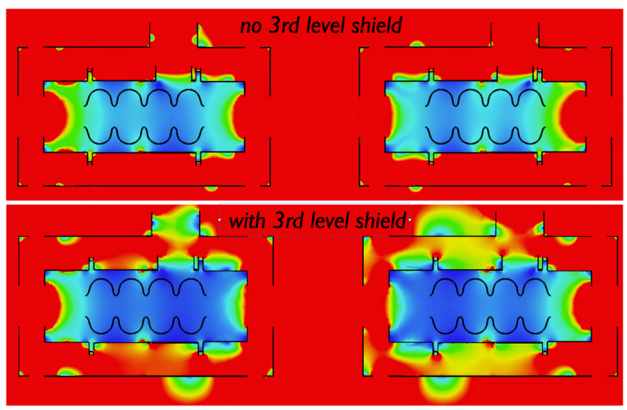

Figure 8: |**B**| for 50 µT ambient exterior field in x-direction, same color scale like Fig. 7.

CONCLUSION

Magnetic shielding of the SRF cavities for VSR Demo is challenging. A fully engineered construction is presented with clearly sufficient attenuation (< 1.0 µT @ 50 µT external) of fields transversal to the cavity axis. A longitudinal field is damped only down to 2.5 µT without and 1.6 µT with an optional 3rd shield layer. Procurement has recently been started, the material choice will be agreed with the vendor.

ISBN: 978-3-95450-227-1 ISSN: 2673-5490 doi:10.18429/JACoW-IPAC2022-THPOST026

REFERENCES

[1] F. Glöckner *et al.*, "The VSR Demo Module Design – a Spaceframe-based Module for Cavities with Warm Waveguide HOM Absorbers", in *Proc. of 20th Int. Conf. on RF Superconductivity (SRF2021)*, East Lansing, MI, USA, Jun.-Jul. 2021, pp. 233-236. doi:10.18429/JACoW-SRF2021-MOPTEV013

[2] A. Jankowiak, J. Knobloch *et al.*, "Technical Design Study BESSY VSR", Helmholtz-Zentrum Berlin, 2015. doi:10.5442/R0001

[3] J. Guo *et al.*, "Development of Waveguide HOM Loads for BerlinPro and BESSY-VSR SRF Cavities", in *Proc. 9th Int. Particle Accelerator Conf. (IPAC'17)*, Copenhagen, Denmark, May 2017, pp. 1160-1163. doi:10.18429/JACoW-IPAC2017-MOPVA130

[4] Salomons Metalen B.V., Datasheet Invar 36. https://salomons-metalen.com/datasheets/Invar_36.pdf

[5] Arcelor Mittal: Stainless & Nickel Alloys., ArcelorMittal_Invar-AM.pdf, 2007.

[6] P. W. Droll, E. J. Iufer, "Magnetic Properties of Selected Spacecraft Materials", NASA Technical Memorandum NASA-TM-X-60414, 1. Jan 1967. https://ntrs.nasa.gov/citations/19680024693

[7] Q. Wei, S. A. Gilder, B. Maier, "Pressure dependence on the remanent magnetization of Fe-Ni alloys and Ni metal", *Phys. Rev. B*, vol. 90, p. 144425, Oct. 2014. doi:10.1103/PhysRevB.90.144425

[8] Simulia CST Studio Suite Vers. 2019.05, Dassault Systems Deutschland GmbH.